

Critical Aerothermal Phenomena on a Future Reusable Booster Stage

Martin Sippel, Josef Klevanski

Space Launcher Systems Analysis (SART), DLR, Cologne, Germany

Ognjan Božić, Hannes Otto

Institute of Aerodynamics and Flow Technology, DLR, Braunschweig, Germany

Frank Tarfeld

Institute of Aerodynamics and Flow Technology, Windtunnel Section, DLR, Cologne, Germany

This paper describes the final design status of a partially reusable space transportation system under study for almost five years within the German future launcher technology research program ASTRA. It consists of dual booster stages, which are attached to an advanced expendable core. The design of the reference liquid fly-back boosters (LFBB) is focused on LOX/LH2 propellant and a future advanced gas-generator cycle rocket motor. The preliminary design study is performed in close cooperation between DLR and the German space industry.

The second part of the paper is devoted to the investigation of the base flow and its interaction with the LFBB's bodyflap. The vehicle's geometry and the seven large rocket engines operating in parallel generate a complex flow field. The engines underexpand at high altitude and the exhaust plume comes into contact with some structural parts, notably the bodyflap. The base flow of the complete launcher configuration during ascent is studied in Euler calculations based on an unstructured grid. Hypersonic windtunnel tests of the LFBB in combination with CFD provide the lift-, drag-, and pitching moment coefficients required for a flight dynamic assessment of the reentry trajectory. Technical options to adapt the reusable booster as well as the expendable core stage for the further improvement of the launch vehicle are discussed.

Nomenclature

D	Drag	N
M, Ma	Mach-number	-
T	Thrust	N
W	weight	N
l	body length	m
m	mass	kg
sfc	specific fuel consumption	g/kNs
q	dynamic pressure	Pa
α	angle of attack	-
γ	flight path angle	-
ε	expansion ratio	-
η	control surface deflection angle	-

TMK Trisonic Test Section (at DLR Cologne)

cog, CG center of gravity

sep separation

1 INTRODUCTION

A reusable booster stage dedicated for near term application with an attached expendable core has been under investigation for almost five years within the system studies of the German future launcher technology research program ASTRA. To date, analysis shows that such a winged fly-back booster in combination with an expendable core stage is technically attractive and is a competitor to other reusable and advanced expendable launchers.

Recently, a System Requirements Review (SRR) has been carried out for this launcher system according to ESA's ECSS standards. The concept is ready now for more detailed investigations in Europe's Future Launcher Preparatory Program (FLPP) along with other potential future European launcher configurations. Among other aspects, critical aerothermal phenomena of the baseflow will be studied.

The examined partially reusable space transportation system of the ASTRA study consists of two booster stages which are attached to the expendable Ariane 5 core stage (EPC) at an upgraded future technology level. The EPC stage is assumed to be powered by a single advanced derivative of the Vulcain engine with increased vacuum thrust. A new cryogenic upper stage (ESC-B-type) should include a new advanced expander cycle motor of 180 kN class (VINCI). Two symmetrically attached reusable boosters, replacing the solid rocket motors EAP in use today, accelerate the expendable Ariane 5 core stage up to separation (Figure 1). All the obtained data of the investigations presented here are easily transferable to launcher configurations including other expendable core stages of similar size. The interest in this kind of space transport is not restricted to combinations with Ariane 5 derivatives.

Subscripts, Abbreviations

BF	Bodyflap
CAD	computer aided design
CAN	Canard
CFD	Computational Fluid Dynamics
CFRP	Carbon Fiber Reinforced Polymer
EAP	Etage d'Accélération à Poudre (of Ariane 5)
ECSS	European Cooperation for Space Standardization
EPC	Etage Principal Cryotechnique (of Ariane 5)
ESC-B	Etage Supérieur Cryotechnique (of Ariane 5)
FEI	Flexible external insulation
FEM	finite element method
FLPP	Future Launcher Preparatory Program
GLOW	Gross Lift-Off Mass
GTO	Geostationary Transfer Orbit
H2K	Hypersonic Wind Tunnel (at DLR Cologne)
JAVE	Jupe AVant Equipée (forward skirt of Ariane 5)
LFBB	Liquid Fly-Back Booster
LH2	Liquid Hydrogen
LOX	Liquid Oxygen
MECO	Main Engine Cut Off
SRM	Solid Rocket Motor



Figure 1: Artists impression of the separation of two attached reusable fly-back boosters from the Ariane 5 core stage

2 TECHNICAL STATUS OF THE RLV BOOSTER

The reusable booster stage propulsion is based on the same advanced version of the EPC's engine, but employs an adapted nozzle with reduced expansion ratio. Three engines are installed in a circular arrangement at the aft of each vehicle. The total length of the latest LFBB variant "Y-9" is almost 41 m. A fuselage and outer tank diameter of 5.45 m is selected so as to achieve a high commonality with Ariane's main cryogenic EPC stage.

Three air-breathing engines, for fly-back, are installed in the vehicle's nose section (see Figure 2), which also houses the RCS and the front landing gear. The nose is of ellipsoidal shape with a length of 6.7 m. The nose section is followed by an annular attachment structure. The structure for canard mounting and actuation is provided at the center of this attachment ring. The cylindrical tank is integral and has the same diameter as the EPC core stage as well as similar lay-out but is shorter in length. This geometry constraint might reduce manufacturing costs if realized, and enables to better compare expendable with reusable structures within this investigation. LOX is stored in the upper portion of the tank and is separated by a common bulkhead from the main LH2 tank. The ascent propellant mass of the latest Y-9 LFBB-configuration is slightly enhanced to 168500 kg without changing the fuselage length. The integral tank section is followed by the wing and fuselage frame section. A second, non-integral LH2 tank is mounted above the wing attachment frames. This tank is interconnected with the main hydrogen tank and it is currently foreseen to feed the engines through this second tank.

The main wing lay-out is based on the transonic RAE 2822 airfoil. The aerodynamic configuration comprises also canards to achieve trimmability in the complete

flight regime. The wing spans about 21 m and its exposed area is about 115 m².

The rocket engines are mounted on a conical thrustframe. A full 2D gimbaling of all engines is required to obtain sufficient controllability of the launch vehicle (see ref. 2). The engines are protected on the lower side by a body flap, with an option to be also implemented for aerodynamic trimming and control. Two vertical fins are attached to the upper part of the fuselage, and inclined at 45 deg. (see Figure 4). The structural support of the complete launch vehicle on the launch table has to be provided by the two LFBB.

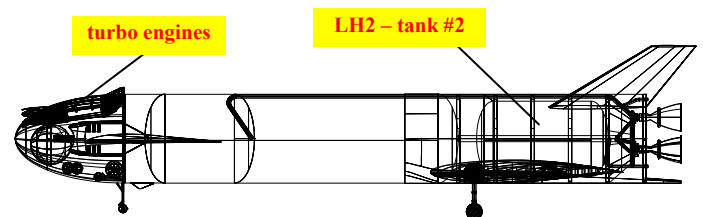


Figure 2: LFBB (Y-9) projection in the x-z-plane

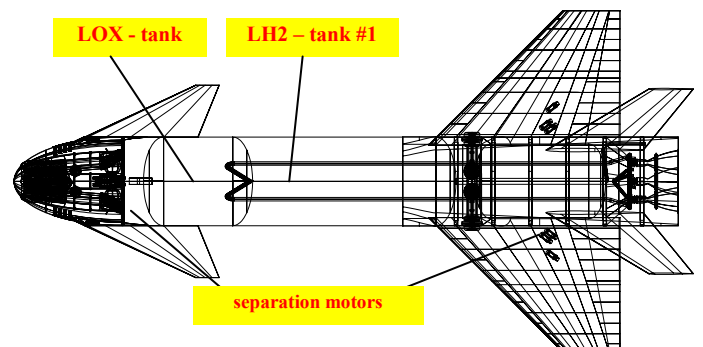


Figure 3: LFBB (Y-9) projection in the x-y-plane

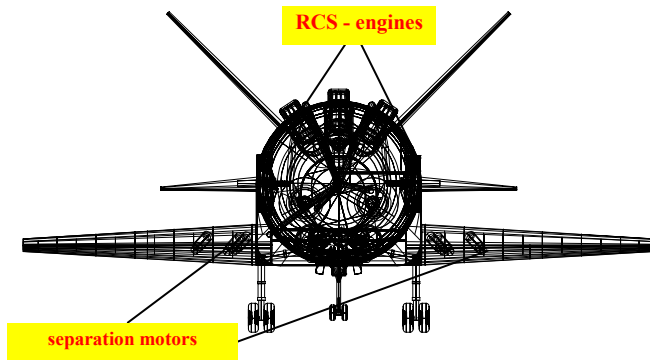


Figure 4: LFBB (Y-9) projection in the y-z-plane

2.1 Propulsion Systems

Four different and independent propulsion systems have to be included in the reusable booster stage:

- Main rocket propulsion
- Fly-back turbofan engines
- Reaction Control System (RCS), and
- Solid separation motors

Advanced cryogenic rocket engines of gas generator cycle type will accelerate the launcher. These might include an increased mass flow and a higher chamber pressure than the recently qualified European Vulcain 2 engine. Although no technical data is yet fixed, the results presented in this paper and in the ASTRA-study are based on assumptions concerning the performance of this motor. These engine data of the variant to be used in the LFBB configuration is given in [3].

Three turbo engines without afterburner which use hydrogen are currently foreseen for fly-back to reduce the fuel mass. The feasibility of replacing kerosene by hydrogen in an existing military turbofan (EJ-200) investigated within the ASTRA-study, shows promising results and no show-stoppers. According to the manufacturer MTU Aero Engines, the installation of the EJ200 *DRY Hydrogen* into the LFBB can be readily achieved by low risk modifications. To limit the costs related to the development programme it is assumed that the majority of existing EJ200 components can be used without modifications and new validation.

The reaction control system (RCS) consists of 10 thrusters on each side of the vehicle with a thrust level of 2 kN per engine. Different propellant combinations are looked upon. Besides the classical but toxic N_2O_4 / MMH, the environmentally friendly GO_2 / Ethanol and GO_2 / GH_2 are possible options. (see ref. 2)

The solid separation motors are located in the attachment ring and inside the main wing structure (see Figure 3 and Figure 4). The design of the motors is derived from the motor lay-out used on the Ariane 5 EAPs but with increased thrust to account for the higher separation mass of the LFBB. Therefore, the propellant grain is elongated by about 64% and the throat diameter is increased by 28%.

2.2 Aerodynamic Design

The aerodynamic work has been carried out at DLR's Institute of Aerodynamics and Flow Technology. The

applied aerodynamic and flight dynamic simulation of the return flight requires trimmed aerodynamic data sets for the complete trajectory from separation at around $M=6$ down to the landing phase at $M=0.27$. The resulting configuration has to comply with tight margins concerning longitudinal stability and trim. Furthermore, the aerodynamic behavior of the booster has to be robust over the complete Mach number range. [4]

The first phase of the aerodynamic design studies, summarized in references 4 and 5, showed the essential need of canards to increase the static margin and to enable the trim of the vehicle. The succeeding work defined a refined aerodynamic configuration of the LFBB. This latest design has a canard with a leading edge sweep of 65° and a trailing edge sweep of 22° . An asymmetric NACA 3408 airfoil is used for the canards. The planform of the large wing is trapezoidal with a 'rear loading' RAE 2822 airfoil.

The resulting vehicle with canards is the basis for the definition of a wind tunnel model. In the meantime this model has been thoroughly investigated in the DLR wind tunnels TMK and H2K (see Figure 5). The force measurements at Mach numbers between $0.6 < M < 7$ have been used to verify the aerodynamic approach. A detailed description of the experimental results is given in ref. 6 and 7.

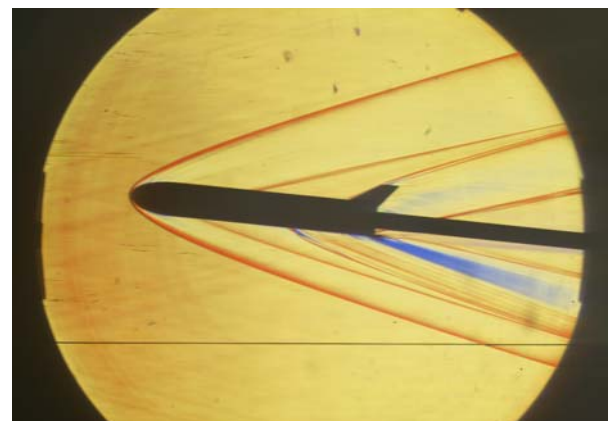


Figure 5: Color Schlieren-technique photo of LFBB Y-7 model in DLR wind tunnel at $M=4$

2.3 Mechanical lay-out of vehicle structure

A preliminary mechanical design of major structural elements is performed. This work is executed by the German launcher industry EADS SPACE Transportation and MAN. The wing, thrust frame, tanks, and fuselage are dimensioned according to the operational loads calculated from flight dynamic and aerodynamic analyses.

The main function of the booster structure is to transfer the thrust to the EPC-stage. Load transferal is foreseen at the forward attachment, in order to keep the same structural architecture as for the EPC of the present Ariane 5. The booster thrust is routed from the thrust frame via the rear fuselage, through the LH2 and LOX tank to the attachment ring structure into the EPC.

At the LFBB's top the nose cap structure is attached which is an aerodynamic cover and houses a large

number of different subsystems (see Figure 6). The turbofans, their secondary LH2 feed tank, the RCS and tanks, the nose landing gear and some avionic subsystems are located inside the nose assembly and are to be supported by the structure.

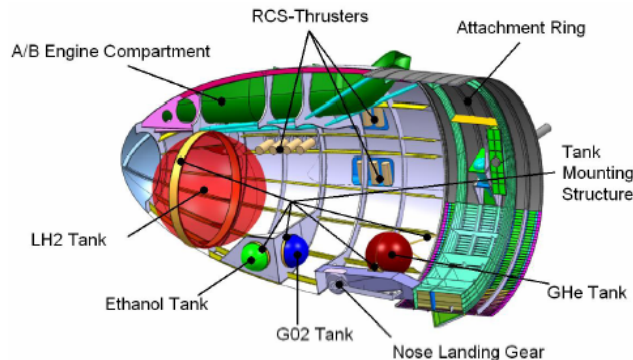


Figure 6: Preliminary design of the LFBB nose and attachment ring showing internal lay-out and some subsystems

The basic design of the booster attachment ring should be analogous to the Ariane 5 EPC forward skirt, but it is especially equipped to satisfy the requirements of a reusable re-entry vehicle. This ring is located between the forward end of the oxygen tank and the LFBB's nose section. It is one of the main structural elements of the booster with very high loads and several interfaces like the canard support and the main attachment fitting, introducing the thrust loads to the expendable core stage. The length of the ring is 2.5 m with the booster's external diameter of 5.45 m.

The forward fuselage consists of an integral, load carrying LH2 and LOX tank and the attachment ring structure. These are designed similar to the Ariane 5 EPC tank and front skirt JAVE. The cylindrical tank parts are integrally stiffened with the stiffeners placed on the outer tank surface. The reference configuration's tanks are to be fabricated from aluminum lithium alloy Al 2195. The rear fuselage is proposed to be made of CFRP, locally reinforced against buckling. (see Figure 7)

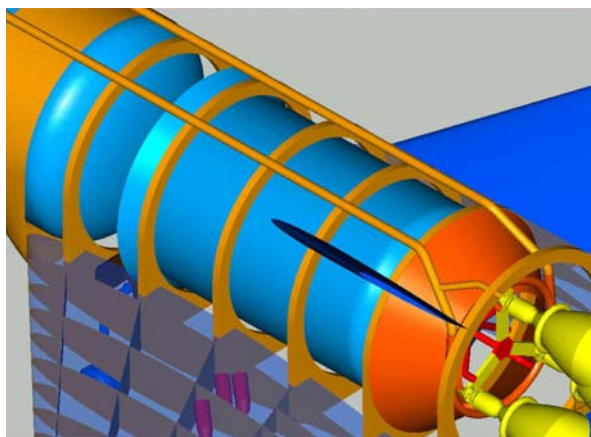


Figure 7: Design of the LFBB rear fuselage structure including the second hydrogen tank as CAD model

The structural concept of the wing consists of a wing box with four spars stiffened with ribs. The shear panels are designed as CFRP sandwich panels, reinforced by T-sections at the lower and upper end. The thrust frame is designed as a conical shell structure, also made of CFRP.

During the reentry flight the booster is subject to moderate aero-thermal heating, never exceeding 100 kW/m^2 at the stagnation point. Nevertheless, the outer skin of the integral tanks with cryogenic insulation and the CFRP body and wing have to be protected against this heat flow. A first analysis of the thermal protection selects a flexible insulation like FEI of different thickness on large part of the vehicle's surface. Another feasible option for the LFBB is a hot structure. However, this alternative approach would require a different mechanical architecture and material selection than that described above.

2.4 Launcher System Analyses and Payload Performance

The usual mission of commercial Ariane 5 flights will continue to be operated from Kourou to a $180 \text{ km} \times 35786 \text{ km}$ GTO with an inclination of 7 degrees. This orbit data and a double satellite launch including the multiple launch structure SPELTRA are assumed. The overall ascent trajectory of Ariane 5 with LFBB is similar to the generic GTO flight path of Ariane 5 with SRM. This trajectory has to respect certain constraints, which are close to those of Ariane 5+ ascent. Throttling of the Liquid Fly-back Booster is not performed, since the Ariane 5 acceleration limit is not reached.

Some characteristic mass data of the investigated LFBB configuration as of March 2005 are listed in Table 1. The dry mass incorporates the results of the detailed structural and subcomponent analyses. The separated satellite payload mass in double launch configuration exceeds 12.3 Mg. The fully cryogenic launcher (boosters, core, and upper stage) is able to deliver almost 2 % of its gross lift-off mass into GTO.

	kg
LFBB dry mass:	46200
LFBB inert (MECO) mass:	54000
GLOW LFBB mass:	222500
GLOW launcher mass:	698850
GTO payload mass (multiple launch):	12330
GTO payload mass (single launch):	13140

Table 1: Characteristic mass data of the Y-9 LFBB launcher with Ariane 5 core stage in GTO mission

All presented data result from an iterative design loop, reflecting the DLR-SART design principles. The ascent trajectory data sets are fully consistent with the corresponding descent and fly-back trajectories. Only converged solution data is presented in this paper.

A quasi-optimal return trajectory is found by parametric variation of the initial banking maneuver [9]. The return of the LFBB should start as early as possible, but is not allowed to violate any restrictions. The banking is automatically controlled to a flight direction resulting in a minimum distance to the launch site. After turning the vehicle, the gliding flight is continued to an altitude of optimum cruise condition.

An elaborate method [9] is implemented to calculate the fuel mass required by the turbojets for the powered return flight to the launch site. The complete flight is controlled

along an optimized flight profile. Aerodynamic data from CFD and windtunnel measurements, vehicle mass, and engine performance (available thrust and sfc) are analyzed in such a way as to determine the stable cruise condition with the lowest possible fuel consumption per range (g/km). This is not a trivial task since engine performance is dependent on altitude and Mach number, and the equivalence of drag-thrust respectively lift-weight is usually not exactly found at maximum L/D. The changing booster mass due to fuel consuming, and a minimum necessary acceleration performance also have to be taken into account.

Including 30% fly-back fuel reserves to take into account possible adverse conditions like head winds, the booster needs about 3.65 Mg hydrogen for its more than one hour return leg. The available propellant margin could be increased compared to earlier simulations [3] due to an improved aerodynamic shape of the refined Y-8 booster. The trimmed hypersonic maximum lift-to-drag ratio reaches a value of about 1.6. In the low subsonic and cruise flight regime trimmed L/D is around 5.5 as has been verified by windtunnel tests. Hypersonic trimming is performed by the canards and supported by the RCS.

3 AEROTHERMODYNAMIC ANALYSIS OF THE LFBB AFT SECTION

From an aerothermal point of view, the booster's aft section is one of the most critical parts of the launcher. The exhaust plume of the LFBB engine cluster and the core stage interact with the external flow. The underexpanding jets at high altitude close to the booster separation interrelate with and contaminate the body flap. Shortening the basic flap design of the Y-8 configuration as it is documented in [3] might be an approach to reduce these interactions. However, the device not only protects the engines during LFBB re-entry but it has also an influence on pitch control in hypersonics which has to be carefully analyzed. Therefore, this paper addresses first the ascent flow analysis, and then the reentry flow conditions from experiment and CFD coupled with a flight dynamic assessment, before options for an even more robust technical solution are proposed.

3.1 Ascent flow analysis

The base flow of the complete launcher configuration during ascent has been studied in Euler calculations for the Y-8 LFBB-configuration using an unstructured grid (see Figure 8 and Figure 9). This unstructured grid is generated with the Centaur Grid Generator from CentaurSoft. The number of tetraeders used in the model described here is approximately 13 million [8].

The external shape of Y-8 is almost identical to the latest Y-9, besides the length of the bodyflap. The engine thrust chamber flow is fully simulated taking into account the chamber pressure and the nozzle contour to achieve realistic nozzle exit conditions. However, the fluid properties are restricted to hot air. An extension to water vapor is foreseen for future analyses. The numerical simulations are carried out with the DLR CFD-solver TAU. Computation time varies from 24 hours to 48 hours for a single flow case of the LFBB launcher [8]. Four characteristic trajectory points have been selected for the

Euler analysis for which the highest at $M_\infty=5.99$ at 54 km altitude (close to the actual LFBB separation) is of special interest in this paper.

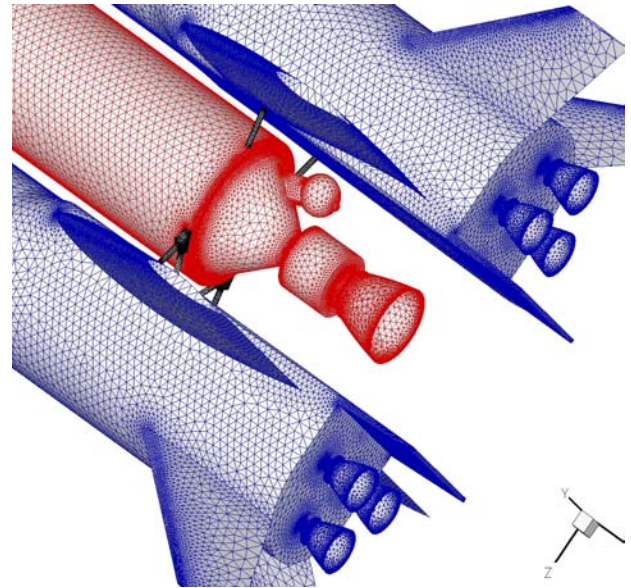


Figure 8: Unstructured grid for the analysis of the launcher's base flow phenomena at the aft section of the Y-8 LFBB configuration

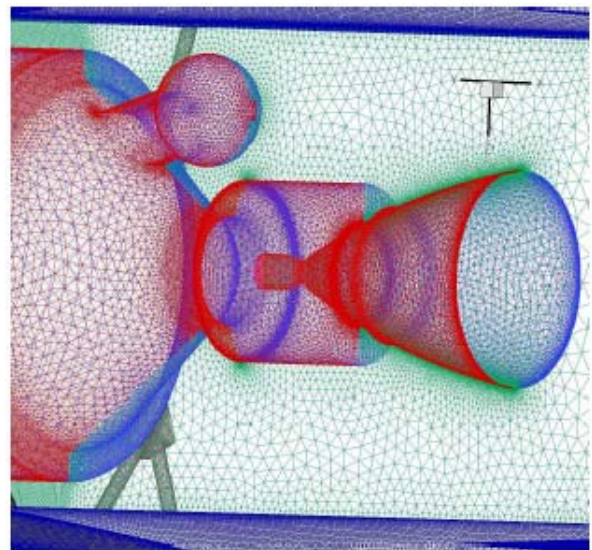


Figure 9: Detailed view of the unstructured grid around the EPC core stage engine

The numerical Euler results allow a comprehensive study of the complicated flow pattern. Flow analysis of the launcher's forward section at different transonic and supersonic Mach-numbers is described in [8]. This paper focuses on the aerodynamic interactions between the Ariane 5 core stage and the two LFBB's in the aft section which is analyzed to particularly address the flow impingement on the body flap. Figure 10 shows the flow field and Mach number distribution at $M_\infty=5.99$ in 54 km, close to the nominal separation point. It can be recognized that the external high pressure tank for helium fixed at the main stage engine thrust frame causes an unsymmetrical flow. Further downstream a reflection with the exhaust jet of the main engine is observed. These phenomena cause unsymmetrical loads at the rearward connecting struts. In comparison with the standard Ariane 5, the effect of the pressurant tank on the

flow conditions is amplified due to the large wings on both LFBB.

The CFD analyses demonstrate that approximately at a flight condition of $M_\infty = 3.5$ in 32 km the core engine's exhaust jet achieves direct contact with the trailing edge of the Y-8 configuration's lower side of the bodyflap. At that point the booster engine plume is still not in contact with this surface. This result is not obvious without calculation because the radial distance of the core engine to the flap is larger than that of the booster engines and it has a considerably lower exit pressure. The latter reaches no more than 8.6 kPa due to the large expansion ratio of 100 using flow separation control, while the booster engines with expansion ratio 35 have an exit pressure of 34.5 kPa. The CFD computation illustrates that the position of the core engine's exit plane, almost 3 m upstream, is the predominant effect. However, with increasing altitude the jets from the lower pair of the booster engines also establish contact with the upper side of the flap. Therefore, it is to be expected that the flap of the Y-8 LFBB will receive heat loads on both side from engine jets. Exit temperature of the core rocket engine is in the vicinity of 1050 K and those of the LFBB engines close to about 1400 K. The temperatures at the contamination points are even lower due to further expansion of the free jets. Thus, the plume contact itself is not a major problem from a materials point of view since the bodyflap and the booster base area has to be thermally protected anyhow.

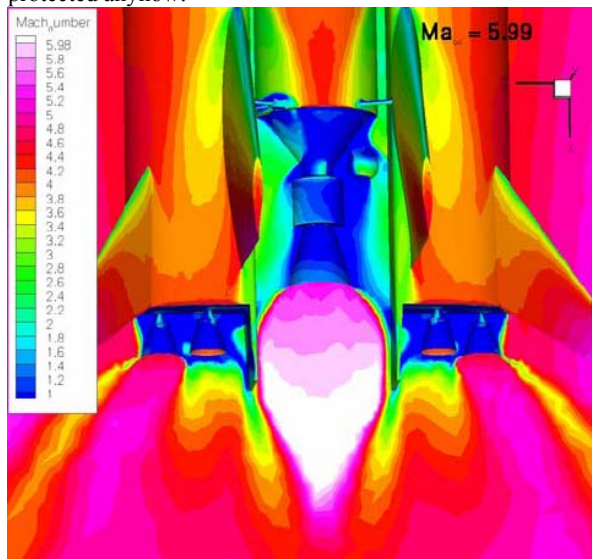


Figure 10: Flowfield and Mach number contours at the launcher's base in the symmetry plane at $M_\infty = 5.99$, $\alpha = 0^\circ$, $\eta_{can} = 0^\circ$ (Euler calculation)

However, the fluctuating pressure distributions and resulting forces and moments on the flat lower side of the LFBB's aft section should be of major concern. The pressure coefficients are calculated up to now for the steady flow condition at $M_\infty = 5.99$. But it is obvious that in reality the rapidly changing flight Mach number and ambient pressure in combination with vortex separations at the aft of the expendable core stage will create strong transient changes in the flow field.

This effect is difficult to be calculated because unsteady 3D-Navier-Stokes computations taking into account the shock boundary-layer interactions are required. Even if detailed and reliable flow data would be available, it

could become extremely challenging to safely control all the three stages at separation.

Following a pragmatic launcher design approach, it is advisable to assess the options of geometric changes on the vehicle. A first measure would be to shorten the flaps' length as long as protection and pitch moment control requirements of the LFBB during reentry could be maintained.

3.2 Descent flow analysis

The reentry flow conditions of the LFBB have been studied in the complete flight regime from hypersonics to subsonics by numerical and experimental methods. A major task of the new windtunnel model of the refined Y-8 configuration which was available in the autumn of 2004 has been used to investigate the influence of different bodyflaps on the vehicle aerodynamics. A detailed description of this windtunnel model is published in reference 7.

The research work has included different bodyflap lengths:

- The original length of 3.25 m as it has been used in the ascent CFD-calculations described in section 3.1.
- A flap of 57 % original length with a trailing edge planar to the nozzle exits of Y-8.
- A configuration without bodyflap ending with the fuselage's trailing edge.

Additionally, different deflections of the full bodyflap and of the canards have been investigated:

- no deflection (0°) of the bodyflap,
- 10° deflection of the bodyflap,
- 30° deflection of the bodyflap, and
- -10° , 0° , $+10^\circ$ deflection of the canards

Figure 11 shows a Schlieren photograph of the LFBB with full length bodyflap and a large 30° deflection in hypersonic flow. Note the detached shocks at the nose, the wing intersection, and the bodyflap.

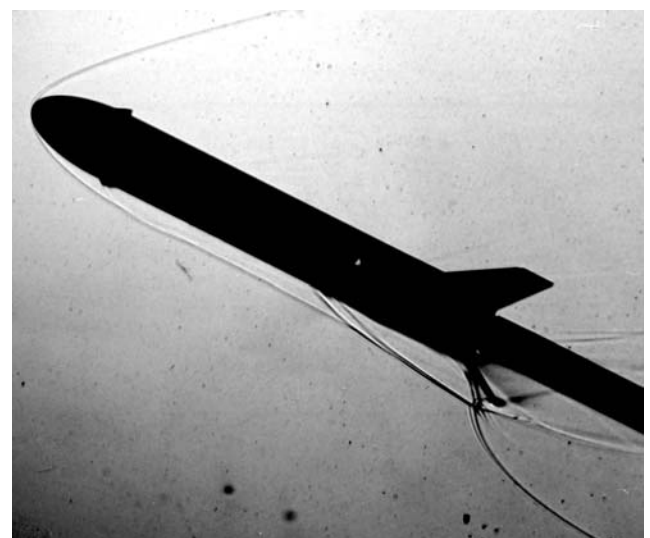


Figure 11: Schlieren-technique photo of LFBB model Y8 in DLR wind tunnel H2K at $M = 6$, $\eta_{CAN} = 0^\circ$, $\eta_{BF} = 30^\circ$, $\alpha = 30^\circ$

The diagram of Figure 12 depicts the influence of the bodyflap deflection and its chord length on the pitching

moment coefficient. The control power of the canards is presented in comparison.

At hypersonic speeds the influence of both control devices is strongly dependent on the angle of attack. The efficiency of the canards is different for positive and negative deflections. At angles of attack below 10° the control power is dominated by the canards, a result which can be found at all investigated Mach numbers, while at higher angles of attack the bodyflap experiences an increasing influence.

Interesting is the pitching moment characteristics with a bodyflap deflection of 30° (see Figure 12). In this case the flow on the windward side of the wing is affected by the strong separated shock upstream of the body flap. This means, that the area with over pressure is larger than the plan form area of the bodyflap alone.

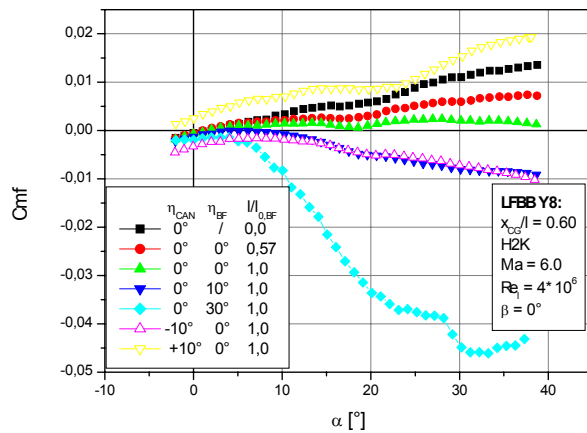


Figure 12: Influence of bodyflap length and deflection as well as canard deflection on pitching moment coefficient c_{mf} at $M = 6$ of LFBB model Y8 in DLR windtunnel H2K

Figure 13 demonstrates that the canards deliver at an angle of attack of 6° a three to four times larger pitching moment than the bodyflap for the same angular deflection. The pitch control efficiency of both devices is enhanced with decreasing flight Mach number. Shortening of the body flap or a complete removal should have no negative effects on trimming the vehicle in hypersonics as long as the canards are not at their operational deflection limit.

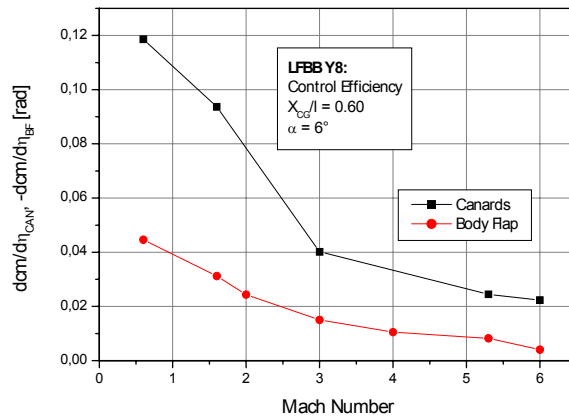


Figure 13: Relative pitching control efficiency of canard and of full bodyflap at $\alpha = 6^\circ$ as a function of Mach number for the LFBB model Y8 in DLR windtunnels TMK and H2K

Figure 12 further shows that canard- and bodyflap deflection as well as bodyflap length has a notable effect on longitudinal stability.

Data from CFD calculations of the Y-8 configuration confirm the findings of the experimental campaign.

3.3 Descent flight dynamic analysis

After receiving numerical and experimental aerodynamic data sets, flight dynamic simulations of the reentry and return trajectory assess the flyability of the aerodynamic configuration. These computations further assess the demand on the size of the two available control surfaces: canards and bodyflap. A complete flight dynamics simulation of the atmospheric reentry and fly-back trajectory is run. Lift-, drag-, and pitching moment coefficients with regard to canard or bodyflap deflection can be used in combination with a calculation of center of gravity (cog) movement, to perform a flight dynamics and control simulation.

The simulations take into account the cog of the booster's latest mechanical architecture and subcomponent distribution. The axial cog is slowly moving forward starting at about 59 % of the reference length. The control aims to keep the normal acceleration factor n_z within 3.5 g and adapts the angle of attack such that the dynamic pressure always stays below 50 kPa.

The flight dynamic simulations are performed with the canards used as the only control devices. A fixed bodyflap on the LFBB is the preferred technical solution because it allows abandoning of a complicated and heavy mechanism and special requirements for thermal protection of breaches. In the simulations the canards show good efficiency under these conditions and can be kept within ± 5.5 degrees of deflection in the nominal flight. Therefore, a generous control margin exists, as the maximum canard deflection might reach at least 10 degrees.

Figure 14 and Figure 15 show the control histories of the LFBB in the most critical hypersonic regime for two different bodyflap lengths. The Mach number range of the figures is between 6 and 1.5. Before 150 s following separation the vehicle is in ballistic flight and the dynamic pressure is very low. The angle of attack should be kept at about 35° when entering the atmosphere.

The flight dynamic simulations reveal notable differences for the two flap variants. The natural stability of the configuration with original bodyflap slightly reduces the angle of attack up to 200 s (see Figure 14). In contrast to this behavior the configuration with shortened flap has become slightly unstable in longitudinal direction and the angle of attack shows the tendency of increasing by a pitch-up maneuver. Note that the vehicle in both cases is in a control loop and the canards are acting against more far reaching discrepancies. After about 200 s the α angle is rapidly reduced by intention to stay within the n_z -limitations. From this point onward the angle of attack differences between both variants almost disappear.

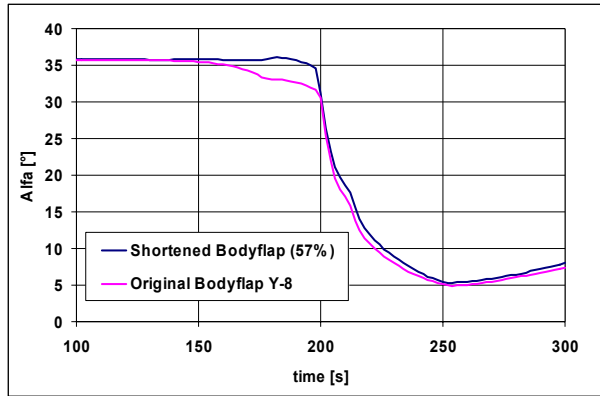


Figure 14: Angle of attack α history from flight dynamic reentry simulation of the LFBB using the original and a shortened bodyflap

Even more striking disparities, as shown in Figure 15, arise for the canard deflection histories. In case of the original design the canards have to redirect by $+5.5$ degrees to counteract the pitch-down movement, while the canards deflect by -1° to counteract the pitch-up rotation of the booster with shortened bodyflap.

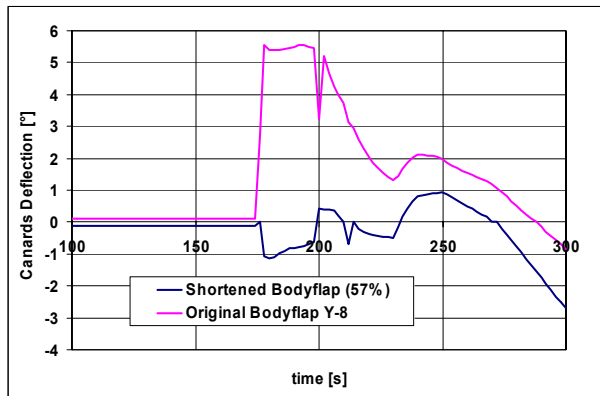


Figure 15: Canard deflection angle η history from flight dynamic reentry simulation of the LFBB using the original and a shortened bodyflap

The flight dynamic investigation proves the flyability of both configurations and once again demonstrates the robust trim behavior of the LFBB with canards. The original configuration shows an almost neutrally stable behavior for $M < 0.8$ and is stable at higher Mach numbers. If the length of the bodyflap is considerably reduced the vehicle with the cog-position at 59% of reference length loses its supersonic and hypersonic longitudinal stability.

None of the dynamic reentry simulations required a movement of the bodyflap. However, the length of this control device is of significant importance for the longitudinal stability. But a safe flight has been demonstrated even under very conservative assumptions on the quality of the actuators and control system.

3.4 Technical options for improvement

The first feasible measure to improve the situation in the base region of the LFBB is to shorten the bodyflap. This can be easily achieved without compromising the protection of the main propulsion system. Therefore, the latest Y-9 booster configuration (depicted in Figure 2 and Figure 3) already introduces this geometry change by

reducing the bodyflap by a length of about 1 m which also offers a mass reduction of more than 100 kg including thermal protection. The actual reduction in length is only by about one-third of the original chord because the main engines have been moved slightly backwards. Although this exact value has not been investigated in the windtunnel the flow phenomena are now quite well understood and the pitching moment coefficients can be easily interpolated for the latest design. The impact of this shortening is acceptable since trimming is always achievable with good margins.

However, the reduced length of the bodyflap is not sufficient to solve all transient heat and pressure problems in the aft region of the launcher. The length and overall geometry of the expendable EPC core stage has been kept frozen during the entire ASTRA-study. This approach allowed of focusing all work on the design of the reusable vehicle. But continuing the design of a sound and technically promising partially reusable launch vehicle no longer requires to maintain this basic assumption. Therefore it seems advisable to lengthen the core stage and to adapt its aft region. By these measures the exit plane of the core engine would move backward close to those of the boosters. An evolution of the existing EPC thrust frame to a more aerodynamically adapted boat tail configuration moreover might offer some major improvements. It should for example enable the reduction of the buffeting loads on the large core stage nozzle in the transonic ascent.

4 CONCLUSIONS

Technical investigations on a partially reusable space transportation system with reusable booster stages, attached to an advanced future derivative of the expendable Ariane 5 core stage, demonstrate the feasibility of several promising design features. The fully cryogenic launcher is able to deliver between 12300 and 13100 kg of payload into GTO depending on the choice of a multiple or single launch configuration.

The reusable boosters are designed with the same external diameter as Ariane5's EPC, the large integral tank is of similar architecture, and the basic lay-out of Ariane 5's forward skirt JAVE is reused for the LFBB's attachment ring. Therefore, existing manufacturing infrastructure might be operated for the RLV assembly. A preliminary design of the structures, major subsystems, and all propulsion systems has been carried out.

Two wind tunnel test campaigns of the LFBB have been successfully concluded. Extensive CFD calculations of the descent and of the ascent vehicle have been performed. An investigation of the launcher's base flow shows that at high altitude, close to the separation point, the underexpanding rocket engine exhaust plume comes into contact with the booster bodyflap. Moreover, critical transient pressure fluctuations on the lower side of the RLV are then to be expected which could become challenging to be safely controlled at separation. Technical measures to significantly improve this situation are investigated. Aerodynamic and flight dynamic analyses of the bodyflap chord demonstrate that a reduction in the length of this device is a feasible

option. Although the configuration might become longitudinally unstable in the hypersonic region, a return trajectory flight simulation demonstrates that under realistic canard actuator conditions the LFBB is fully controllable by active means.

Moreover, an evolution of the existing expendable stage with increased length and an adapted thrust frame with aerodynamically optimized tail body might offer some major improvements. This approach ultimately enables the optimization of the complete expendable core stage.

The ASTRA investigation of the last five years gives evidence that a semi-reusable launcher is a robust and flexible space transportation system. All applied technologies of the LFBB-RLV are well within reach in the next 10 years. The reusable stage can be used to support the transportation to orbit of a very broad range of payload masses as has been previously demonstrated. Therefore, reusable booster stages represent an interesting and serious option in the future European launcher architecture.

5 ACKNOWLEDGEMENTS

The authors gratefully acknowledge the contributions of Mrs. Uta Atanassov, Ms. Chiara Manfletti, Mr. Holger Burkhardt, and Mr. Armin Herbertz and those from the ASTRA joint industry-DLR team who contributed to the preliminary sizing of the Liquid Fly-Back Booster.

6 REFERENCES

1. Sippel, M.; Atanassov, U.; Klevanski, J.; Schmid, V.: First Stage Design Variations of Partially Reusable Launch Vehicles, J. Spacecraft, V.39, No.4, pp. 571-579, July-August 2002
2. Sippel, M.; Klevanski, J.; Burkhardt, H.; Eggers, Th.; Božić, O.; Langholf, Ph.; Rittweger, A: Progress in the Design of a Reusable Launch Vehicle Stage, AIAA-2002-5220, September 2002
3. Sippel, M.; Manfletti, Ch.; Burkhardt, H., Eggers, Th.: Technical Development Perspective of Reusable Booster Stages, AIAA 2003-7057, December 2003
4. Sippel, M.; Klevanski, J.: Preliminary Definition of an Aerodynamic Configuration for a Reusable Booster Stage within Tight Geometric Constraints, 5th European Symposium on Aerothermodynamics for Space Vehicles, November 2004
5. Eggers, Th.: Aerodynamic Design of an Ariane 5 Reusable Booster Stage, 5th European Symposium on Aerothermodynamics for Space Vehicles, Cologne, November 2004
6. Tarfeld, F.: Experimental Study on a Liquid Fly-back Booster Configuration in Windtunnels, AIAA-2003-7056, December 2003
7. Tarfeld, F.: Comparison of two Liquid Fly-Back Booster Configurations based on Wind Tunnel Measurements, 5th European Symposium on Aerothermodynamics for Space Vehicles, Cologne, November 2004
8. Božić, O.: Flow Field Analysis of a Future Launcher Configuration during Start, 5th European Symposium on Aerothermodynamics for Space Vehicles, Cologne, November 2004
9. Klevanski, J.; Sippel, M.: Quasi-optimal Control for the Reentry and Return Flight of an RLV, 5th International Conference on Launcher Technology, Madrid November 2003

Further updated information concerning the SART space transportation concepts is available at:
<http://www.dlr.de/SART>